HHS Public Access

Author manuscript

Biomaterials. Author manuscript; available in PMC 2016 May 01.

Published in final edited form as:

Biomaterials. 2015 May ; 49: 9–17. doi:10.1016/j.biomaterials.2015.01.027.

Development of a Biological Scaffold Engineered Using the Extracellular Matrix Secreted by Skeletal Muscle Cells

Shiloh Hurd, **Nadia Bhati**, **Addison Walker**, **Ben Kasukonis**, and **Jeffrey C. Wolchok**

Department of Biomedical Engineering, College of Engineering, University of Arkansas

Abstract

The performance of implantable biomaterials derived from decellularized tissue, including encouraging results with skeletal muscle, suggests that the extracellular matrix (ECM) derived from native tissue has promising regenerative potential. Yet, the supply of biomaterials derived from donated tissue will always be limited, which is why the *in-vitro* fabrication of ECM biomaterials that mimic the properties of tissue is an attractive alternative. Towards this end, our group has utilized a novel method to collect the ECM that skeletal muscle myoblasts secrete and form it into implantable scaffolds. The cell derived ECM contained several matrix constituents, including collagen and fibronectin that were also identified within skeletal muscle samples. The ECM was organized into a porous network that could be formed with the elongated and aligned architecture observed within muscle samples. The ECM material supported the attachment and in-vitro proliferation of cells, suggesting effectiveness for cell transplantation, and was well tolerated by the host when examined in-vivo. The results suggest that the ECM collection approach can be used to produce biomaterials with compositions and structures that are similar to muscle samples, and while the physical properties may not yet match muscle values, the in-vitro and in-vivo results indicate it may be a suitable first generation alternative to tissue derived biomaterials.

1. Introduction

When provided with the appropriate cues muscle has a robust capacity for self repair. Following mild muscle damage (ex. strains, contusions, and lacerations) cells may be injured, but the underlying extracellular matrix (ECM) is largely intact and repair is robust [1, 2]. However, when significant muscle volume is lost (trauma or surgical resection) the physical and chemical cues provided by the ECM are absent and the defect is instead replaced with non-contractile scar tissue [3]. The current standard of care to replace severely damaged or missing muscle is the transfer of autologous muscle flaps. Flap transfers have been used to reconstruct human forearm, elbow, and shoulder muscles [4–6]. Yet, the transfer of muscle tissue is an invasive procedure that causes significant donor site

Corresponding Author: Jeff Wolchok, 125 Engineering Hall, Department of Biomedical Engineering, University of Arkansas, Fayetteville, AR 72701, jwolchok@uark.edu, 479 575-2850, 479 575-2846.

morbidity, and is therefore only rarely indicated. As an alternative to muscle flap transfer, scaffolds or similar bulk implants could be utilized to guide skeletal muscle regeneration within a defect site.

With this goal in mind, several past and recent research efforts have focused on the development of skeletal muscle scaffolds fabricated using synthetic polymers [7–9]. Unlike muscle flaps transfers, synthetic scaffolds can be produced in nearly unlimited quantities and eliminate the complications associated with donor site morbidity. However, the use of synthetic scaffolds for the repair of damaged skeletal muscle has not yet shown clinical promise and appears unlikely to replace flap transfers in the clinical setting. A potential roadblock to the use of synthetic scaffolding for skeletal muscle repair is the foreign body reaction that is directed against all synthetic polymers including degradables. In an effort to evade the foreign body response, more recent efforts have shifted away from synthetic implants and towards tissue derived ECM that can be remodeled by the body's own wound healing machinery [10–13].

Towards this end, the development of ECM scaffolds derived from decellularized skeletal muscle (DSM) tissue has been explored. The multi-molecular properties of tissue derived ECM gives these naturally derived biomaterials a level of complexity and remodelability not observed with synthetic materials [14, 15]. In fact, significant research effort has been focused on mimicking the properties of ECM in synthetics [16–18], suggesting recognition of the important role of ECM molecules during the wound healing process. Additionally, DSM biomaterials can be produced from allogeneic tissue, thereby eliminating concomitant donor site morbidity. Most importantly, the performance of DSM implants for the repair of skeletal muscle defects has shown promise. When used for the repair of hind-limb muscles in a rat model, decellularized muscle scaffolds were capable of restoring contractile force measurements to 85% of pre-injury levels [19]. Similar encouraging regeneration results have been reported by others using muscle derived ECM scaffolds [20, 21]. When viewed as a whole, the tissue derived ECM repair results suggest that these materials can provide the vital cues needed to regenerate volumetric muscle defects. While donated human tissues are the current gold standard we suggest that an engineered ECM (eECM) biomaterial that provides the appropriate regenerative cues by mimicking many of the key properties of DSM is an attractive alternative worth investigation.

To create eECM biomaterials we are exploring methods to farm the ECM that is secreted by populations of cells during growth in culture. While methods to collect isolated molecules from cells in culture have existed for some time, for example hybridoma cells are routinely used to produce antibodies [22], the wholesale collection of cell secreted ECM proteins provides a means to create bulk biomaterials. To collect the ECM that cells secrete, our group has developed a solvent degradable sacrificial foam fabricated from medical grade polyurethane [23]. The scaffold's are used in a manner that is analogous to the use of honeycombs to collect the honey secreted by bees. We have demonstrated that when cells are seeded onto the scaffolds and grown in culture they secrete a multitude of ECM molecules that accumulate within the scaffolds open spaces. The innovative step is that the sacrificial scaffold can be thoroughly dissolved using a water miscible solvent, stripping away the synthetic component and leaving behind only the accumulated ECM. The result is

a bulk eECM biomaterial comprised of the molecules secreted by living cells. This report describes the application of our ECM collection process to create an eECM scaffold constructed from the molecules secreted by cultured skeletal muscle cells, as well as comparisons of the material to DSM samples.

2. Methods

Decellularized Skeletal Muscle Preparation

Gastrocnemius muscle (n=10) was collected from commercially purchased (Harlan, Indianapolis, IN) Sprague Dawley rats (>300g) that had been previously euthanized as part of an unrelated study. All animal procedures were performed in accordance with protocols approved by the University of Arkansas Institutional Animal Care and Use Committee (IACUC). Harvested muscle was decellularized following a published protocol [24]. Tissue was rinsed for 90 min in Tris-HCL (10mM, pH 8.0) with 1% EDTA and 10kU/ml aprotinin at 4°C with agitation. Samples were then soaked in 1% sodium dodecyl sulphate (SDS) in Tris-HCL buffer for up to one week at room temperature using gentle agitation. To remove nuclear remnants, samples were incubated for 24 hours in reaction buffer containing 50U/mL deoxyribonuclease I and 1U/mL ribonuclease A in phosphate buffer saline (PBS; pH 7.4) at 37°C with agitation. Samples were rinsed in PBS, (pH 7.4) for 48 hours (4°C) with multiple rinses to remove any residual decellularization solution, frozen (−80°C), and lyophilized to preserve tissue structure. DSM samples were weighed and yield was calculated relative to undecellularized muscle volume ($mg/cm^{3)}$).

eECM Sample Preparation

Open celled polymeric sacrificial foams were fabricated from a medical grade polyurethane elastomer (Tecoflex, Luibrizol, Wickliffe, OH) using a granular sugar templating process (see supplemental data). To form the sugar templates, approximately 5g of granulated culinary table sugar (sucrose) was mixed thoroughly with 100ul of distilled-deionized (DD) water to create a lightly moistened sugar slurry. The sugar slurry was packed into disk shaped molds (30mm diameter × 3mm thickness) and incubated at 50°C for 20 minutes to remove the residual water and create a hardened sugar template. Polyurethane (PU) pellets were dissolved in dimethyacetamide (DMAC) (10% w/v) overnight at 50°C and then pipetted into sugar templates. Polymer soaked templates were immersed overnight in a room temperature DD water bath, which both precipitated the PU solution and dissolved the sugar template. The PU foams were rinsed in DD water at room temperature for 48 hours to remove any residual sugar and solvent, frozen (−80°C), and lyophilized for long term storage.

Commercial rat skeletal muscle myoblasts (L6, ATCC, Manassas, VA) were expanded *in-vitro* following supplier guidelines and seeded onto sacrificial foams at a concentration of 4 million cells per cm^3 of foam. Prior to cell seeding, all sacrificial foams were incubated overnight at 4°C in a fibronectin solution (20ug/ml) to facil itate cellular attachment. Cell seeded sacrificial foams were maintained in growth media consisting of DMEM-F12 supplemented with 10% FBS, 1mM ascorbic acid, and transforming growth factor beta1 (TGFβ1, PeproTech, Rocky Hill, NJ) at a concentration 0.5 ng/ml to accelerate cellular

ECM production. Cell seeded foams were maintained in culture for 4 weeks. Cultivation conditions utilized during this study were established during preliminary pilot testing (see supplemental data). Growth media was exchanged every 48 hours. At the completion of the culture period, samples were rinsed in DD water and incubated in DMAC for at least 72 hours at room temperature to remove the sacrificial PU foam. The solvent was exchanged 4 times during the 72 hour incubation period, twice on the first day and then daily thereafter. The remaining cell derived material was collected, rinsed in DD water, decellularized as previously described, and characterized in comparison with DSM samples.

Imaging

DSM and eECM samples (n=5/sample group) were fixed overnight in 4% paraformaldehyde, paraffin embedded, and sectioned with a microtome (10um). Sections were mounted onto slides, stained with hematoxylin and eosin (H&E), and microscopically imaged (100X). Three representative images from each sample were used to measure porosity (% open space), pore size (mm^2), and pore alignment (average oriented angle) using image analysis software (ImageJ) and guided by published techniques [25, 26]. For DSM sample image analysis, the direction of muscle contraction (long axis of the gastrocnemius muscle) was selected to correspond to an orientation angle of 0 degrees. Additionally, bulk eECM and DSM samples, as well as cell free sacrificial foams were lyophilized, sputter coated with platinum, and imaged with the aid of a scanning electron microscope.

To visualize accumulated ECM proteins within DSM and eECM samples, mounted sections were immune-reacted for the presence of collagen type I (αrat collagen 1, mouse IgG1, 750:1, Sigma, St. Louis MO) and cellular fibronectin (αrat cellular fibronectin, mouse IgM, 400:1, Sigma, St. Louis MO) followed by incubation with the appropriate fluorescently labeled secondary antibodies (500:1, Invitrogen, Carlsbad, CA). Sections were counterstained with the nuclear staining reagent DAPI, and then microscopically imaged.

Mechanical Testing

DSM and eECM mechanical properties were measured with the aid of a uni-axial tensile tester (UStretch, CellScale, Ontario, Canada) using techniques familiar to our group [27–29]. Prior to testing, samples (n=4/sample group) were imaged and cross-sectional area was calculated using image analysis software (ImageJ, NIH, Bethesda, MD). Hydrated (PBS, pH=7.4) samples were deformed at a constant strain rate of 1%/s until failure using a 0.5N load cell while the load and displacement values were recorded. For each sample, engineering stress versus strain curves were generated from load and elongation data. Strain was determined using grip displacement values. From each curve the tangent modulus was calculated from a linear fit to the stress-strain curve.

Composition

Collagen content for both DSM and eECM samples was estimated from hydroxy-proline concentration. Hydroxy-proline concentration was determined from extracted samples (n=4/group) using a published technique [30]. Briefly, extracted samples were digested in a 6N HCL solution (4 hrs at 110°C) and then neutralized with sodium hydroxide. Digested

samples were mixed with a chloramine T solution (1:2) and incubated at room temperature for 20 minutes. A dimethyl-aminobenzaldehyde assay solution was added (1:2) and the mixture was incubated at 60°C for 15 minutes. During this time a red chromophore develops. Chromophore intensity indicates hydroxy-proline concentration. Sample absorbance was read at 550 nm using a microplate reader. DSM and eECM values were compared against a standard curve, and collagen concentrations were calculated.

To broadly characterize the protein fingerprint, a representative eECM sample was analyzed with tandem mass spectroscopy (MS/MS). The sample was washed with 50mM ammonium bicarbonate, denatured (Protease Max, Promega, Madison, WI) for 30 minutes at room temperature, trypsin (20ng/μl) digested overnight at 37°C, and purified (Ziptip, Milipore, Billerica, MA). The MS/MS analysis was performed under the direction of the University of Utah proteomic core facility using a hybrid mass spectrometer (LTQ-FT, Thermo Scientific, Waltham, MA). Primary peptide molecular mass spectra were acquired by Fourier transform ion cyclotron resonance. The sequencing of individual peptide spectra was performed by collision induced dissociation in the linear ion trap. Sample proteins were identified by comparison of MS/MS measured peptide sequences to a trypsin-cut specific protein database (Mascot ver. 2.2.1, Matrix Science Inc., Boston, MA).

In-Vitro and in-Vivo Biocompatibility

A direct contact assay was employed to assess cellular attachment and proliferation upon eECM materials. Engineered ECM material islands (diameter = 5mm) were created on glass microscope slides. Engineered ECM islands were seeded with skeletal muscle myoblasts (L6, ATCC, Manassas, VA) at a density of 5K cells per island. Cell viability was evaluated at 2, 5, 7, and 11 days (n= 4 islands/day) using calcein AM (Life Technologies). Five representative fields were imaged (100x) from each island and captured digitally. From the digital images, average cell confluency (% surface area) was calculated at each time point with the aid of image analysis software (ImageJ).

In-vivo host response was examined using a dorsal subcutaneous implant site. *In-vivo* biocompatibility was assayed at short-term (4 weeks) and long-term (12 weeks) time points. Mature male Sprague Dawley rats (300+g) were used (Harlan, IN). All surgical procedures were performed in accordance with protocols approved by the University of Arkansas Institutional Animal Care and Use Committee. Anesthesia was induced using isoflurane (2–4%) in oxygen. The subcutaneous implant site was surgically exposed through a 2 cm left-right incision placed 2 finger widths caudal to the scapulae. A subcutaneous pouch was created in each animal by blunt dissection. A single DSM or eECM sample was implanted into each pouch (approximate implant size 10mm diameter). Incisions were closed using surgical adhesive (VetBond, 3M). Following surgery all animals were housed in the University of Arkansas Central Laboratory Animal Facility. At the prescribed time-points (4 and 12 weeks) all animals (n=3/timepoint) were euthanized via inhalation of carbon dioxide. The implant site with surrounding soft tissue was harvested, fixed in 4% paraformaldehyde, paraffin embedded, sectioned (10um), and stained with H&E. Stained sections were imaged and examined for evidence of inflammation and material degradation.

Oriented eECM Sample Preparation

To explore the affect of sacrificial foam architecture on the structure of eECM material collected from it, sugar templates with muscle inspired alignment were fabricated using drawn sugar fibers. Culinary table sugar granules were heated to 280°C to create a viscous melt, from which elongated sugar fibers were hand drawn (average diameter=0.59±0.2mm). Bundles of elongated sugar fibers were packed into molds, saturated with 10% PU solution, and incubated overnight in DD water to produce drawn fiber sacrificial PU foams. The drawn sugar sacrificial foams (n=6) were seeded with L6 myoblasts (4×10^6 cells/cm^3) and cultivated for four weeks using standard growth media supplemented with TGFβ1 (0.5 ng/ml) and ascorbic acid (1 mM). All cultivation parameters were consistent with previously described granular sugar sacrificial foam eECM sample preparation. At the completion of the cultivation period, the eECM material was collected and material alignment (average orientation angle) was determined from image analysis of histologic thin sections (10μm) as previously described.

Data Analysis

All data is represented by the mean and standard deviation. Comparisons between DSM and eECM material properties (yield, moduli, architecture, and collagen content) as well as animal growth rates were evaluated using a student's t-test. The relationship between culture duration and average cell confluency was evaluated with single factor ANOVA. Post hoc comparisons were made using Tukey's test. A standard 0.05 level of significance was used for all statistical tests.

3. Results

Bulk eECM samples isolated from myoblast seeded sacrificial foams exhibited a white and lacy appearance visually similar to that observed for DSM samples (Figure 1). Decellularized rat gastrocnemius skeletal muscle yielded 18.5±5.2 mg of DSM material for every cm^3 of muscle harvested, a yield value that represents approximately 10% of the native skeletal muscle weight. Average eECM material yield using skeletal muscle derived myoblast cells was 6.8±1.7mg collected for every cm^3 of cell seeded sacrificial foam, or approximately 37% of DSM yield values. Both eECM and DSM samples are highly porous and defined by a bulk network of cell derived material (Figure 2). eECM materials were significantly more porous than DSM materials. On average eECM materials were 21% more porous than DSM samples, a finding that is consistent with the differences measured between eECM and DSM yield values. The individual fibers within the DSM network are generally aligned in an orientation that is consistent with the direction of muscle contraction. Alternatively, eECM materials retain a more randomized network structure that is consistent with the granular architecture of the open spaces within the sacrificial PU foam from which it was collected. Additionally, the average size of the pores within eECM samples was significantly smaller than DSM samples.

Both DSM and eECM samples were tough enough to withstand handling and tensile testing. Stress versus strain curves for both materials were characterized by a short toe-in region (out to approximately 5%) followed by a nearly linear ($R^2>0.9$) increase is stress extending out

to failure at approximately 25% for eECM materials and 50% for DSM samples (Figure 3). Comparable stress versus strain patterns were observed for each sample tested. Similar to material yield results, average DSM sample elastic moduli were three times greater than eECM values. The average tangent modulus measured within the linear stress strain region was 172±25kPa and 50±24kPa for DSM and eECM samples respectively. The difference between DSM and eECM elastic modulus values was statistically significant.

The accumulated eECM material was robustly immunoreactive to both collagen type 1 and fibronectin (Figure 4). Although present at measurable quantities within eECM samples, the collagen content of eECM samples as determined by hydroxyl-proline analysis, was approximately 20% of DSM values. The presence of fibronectin and collagen type 1 as well as collagen types III, VI, and XII within eECM samples was also identified via tandem mass spectroscopy. The presence of additional eECM proteins including laminin, decorin and thormbosponsdins 1 and 2 were also identified via tandem mass spectroscopy.

The eECM samples were cyto-compatible and supported the attachment and *in-vitro* proliferation of cultured myoblast cells. Forty-eight hours after seeding, viable cells covered, on average, 8±5% of eECM sample surface (Figure 5). Myoblast cell surface coverage continued to increase by approximately 10% for each additional day in culture suggesting active proliferation. By five days post seeding, cell coverage increased to 25±10% of the eECM sample surface and by eleven days cell coverage had nearly reached confluency (84% ±8%). Cells cultured on eECM materials appeared well spread with morphologies similar to that observed for cells seeded onto tissue culture treated polystyrene surfaces, yet unlike synthetic polymer surfaces, the eECM material did not require surface treatment to promote cell attachment.

All implanted animals tolerated the implantation surgery well and gained weight throughout the observation period at a rate (8.6±1.6 grams/week) that was not significantly different from un-implanted controls (9.1±1.8 grams/week). At four weeks post implantation, eECM materials were well incorporated into the surrounding tissue and host cells had densely penetrated the material (Figure 6). The dense cellular penetration into the eECM material was suggestive of active remodeling of the implant site. There was no evidence of a dense fibrous encapsulation layer surrounding eECM materials nor was there any evidence of multinuclear giant cell formation in regions surrounding the implants. By twelve weeks post implantation, eECM materials were completely degraded and appeared qualitatively similar to no implant controls. No evidence of residual material could be identified in any of the implanted animals. There was no evidence of local or systemic toxicity to eECM materials, nor any evidence of chronic inflammation at any of the implantation sites.

Sacrificial foam architecture significantly influenced both the amount and structure of the eECM collected. While bulk eECM materials were successfully collected from all cell seeded drawn fiber sacrificial foam samples tested, the eECM yield (1.8±0.3 mg/cm^3) was significantly less than that measured for granular sugar foams (6.8±1.7 mg/cm^3). However, the eECM collected from drawn fiber foams showed strong evidence of material alignment with an average dominant oriented angle of 2.8±2°, which is consist ent with the direction (designated as 0°) of sugar fiber alignment (Figure 7). The orientation angle was

significantly different from eECM materials collected from granular sugar template foams, which showed little evidence of network alignment (32±8°). The orientation of eECM material collected from drawn fiber foams was more consistent with DSM samples, which all had an ECM network closely aligned (11±5°) with the direction of muscle contraction (designated as 0°).

4. Discussion

In patients with tissue injuries that require replacement rather than repair, the gold standard treatment remains tissue transplantation. Unfortunately, the number of patients that can benefit from transplantable tissues is far greater than the supply. For instance, although approximately 100,000 cornea transplants are performed around the world each year [31], it is estimated that up to 5 million people could benefit from this procedure [32]. Similar shortages exist for other tissue types [33, 34]. To meet demand, alternatives to donated human tissues must be identified and developed. An engineered approach to the creation of biomaterials that mimic tissue has long been considered a viable solution. Towards this end, our group is interested in the development of eECM biomaterials that are targeted for the repair of damaged skeletal muscle. As a first step towards this goal, we have developed a “cellular beekeeping” approach to collect the ECM secreted by muscle cells during growth in culture. This bottom-up fabrication strategy is predicated on a basic idea; cells already have the necessary machinery to create ECM biomaterials, we just need to develop platforms to effectively capture the molecules that they secrete. To guide our development efforts, we also measured the chemical, mechanical, and structural properties of skeletal muscle ECM prepared using a top-down decellularization approach. These values serve as a design template that can be used to make quantitative comparisons between engineered and native muscle samples which could then be used to guide next-generation material refinements.

A notable difference between the eECM synthesis approach and the collection of ECM from skeletal muscle is reduced material yield. Under optimized conditions approximately 7mg of eECM was produced for every square centimeter of sacrificial foam seeded with cells, or approximately one-third the yield measured from skeletal muscle samples. To improve yield the application of mechanical stimulation during cultivation could be utilized to increase cellular ECM production, although our experience with mechanical bioreactors suggests that only modest improvements would be expected [28, 35]. Rather than enhancing the cellular production of ECM during cultivation, an alternate strategy could be improving the retention of the ECM that is produced within the sacrificial scaffolds. We recognize that much of the ECM secreted by the cells during *in-vitro* cultivation is not fully captured by the sacrificial foams and is instead lost during media exchanges. Within native tissues, cells are embedded within the ECM which limits the diffusion of secreted ECM away from the site of production. Alternatively, cells in culture are in a unique environment with minimal surrounding ECM. To better replicate the *in-vivo* environment, the creation of a diffusion limiting crowded space through the addition of molecular crowding molecules into the growth media has been shown to accelerate ECM accumulation by fibroblast cells in culture by as much as 18-fold [36]. Another option to limit diffusion is physical encapsulation of the sacrificial foams using porous filtration membranes. Appropriately designed membranes

would permit adequate nutrient exchange, but would restrict the escape of large (i.e. collagen) ECM molecules during media changes. The application of diffusion limiting techniques to enhance ECM collection is not just relevant to the eECM synthesis process described in this manuscript, but could also be used to enhance ECM accumulation in cell based tissue engineering approaches.

Like yield, the modulus of eECM samples was approximately one-third that of DSM materials. The difference may be a direct result of the reduced yield and increased porosity of eECM materials when compared to DSM samples, but may also reflect fundamental differences in eECM and DSM composition and organization that were not revealed during characterization activities. Although the values are different, the impact of a mechanical property mismatch between eECM and DSM materials on *in-vivo* regenerative performance is potentially minimal. Recently published muscle regeneration results using a minced muscle implant slurry suggest that initial restoration of implant site mechanical integrity was not required to achieve regeneration [37]. When packed into critically sized rat skeletal muscle defects, the finely minced muscle grafts promoted substantial regeneration of innervated muscle fibers within the defect site, as indicated by de-novo muscle fiber regeneration and improved force production. The minced muscle graft provided negligible mechanical restoration, which suggests that the essential design element for successful regeneration may not be mechanical, but is instead the stable delivery of key ECM molecules and regenerative cells into the defect site. The encouraging skeletal muscle regeneration results reported by others using decellularized bladder and intestinal implants, tissues with mechanical properties different from muscle, support this hypothesis [38, 39]. This suggests that a successful material may primarily serve as a bulking agent or filler that provides a stable and cytocompatible delivery platform for the appropriate regenerative cell population as well as a reservoir of key wound healing growth factors that are known to reside within native muscle tissue. While not measured in this study, we have identified the presence of growth factors and signaling molecules within eECM materials derived from other cell types [23], and if necessary key molecules could be linked to myoblast derived eECM materials prior to implantation [40].

The demonstrated cytocompatibility and proliferative environment provided by eECM materials is encouraging. The cytocompatibility results suggest that eECM materials described in this study could support not only the infiltration of native regenerative cells following implantation, but also the co-delivery of progenitor cells during implantation. The successful co-delivery of progenitor cells has been shown to significantly improve the functional regeneration of skeletal muscle injuries in not just the minced muscle model, but also with DSM and decellularized bladder ECM implants [19, 41]. With these results in mind, progenitor cell co-delivery will likely become an integral part of any future eECM based regenerative approach. Various progenitor cell sources have been considered, including delivery of the same myoblasts used to create the eECM materials. However, the most likely translatable approach is the co-delivery of bone marrow derived mesenchymal stem cells (MSCs). Bone marrow is a rich source of MSCs that are known to have myogenic potential [42] and contribute to the repair process following muscle injury. Additionally, MSC delivery could enhance the regeneration of vessels and nerves. With this goal in mind,

our preference is to maintain cell “stemness” prior to implantation. Currently, the *in-vitro* results suggest that myoblasts can attach to and proliferate upon eECM materials. The potential influence of eECM attachment on differentiation, particularly upon aligned materials, is unknown and warrants exploration.

While the importance of implant mechanics on *in-vivo* performance is unclear, we as well as others anticipate that biomaterials with muscle mimetic network alignment might improve muscle regeneration by providing the appropriate topographical cues during healing [43, 44]. With this in mind, we were interested in developing approaches to fabricate eECM scaffolds with muscle like structure using the sacrificial foam approach. The ECM derived from native muscle tissue is aligned in the direction of muscle contraction and surrounds multi-nucleated myocytes that are from 5 to 100um in diameter and can be as long as several centimeters [45]. To create eECM biomaterials with muscle mimetic architecture the relationship between sacrificial foam structure and the eECM collected within it was explored. During early development efforts it was observed that the structure of the eECM material that is collected from the sacrificial foams resembles the structure of the foam itself. Similar in concept to a molded part, the ECM that accumulates within sacrificial foams takes on the architecture of the void space and retains this shape when the foam is dissolved. To create foams with muscle mimetic structure, we explored a drawn sugar templating method. Instead of using granulated sugar to create sacrificial foams with spheroid pores, drawn sugar fibers were used to create sacrificial foams with aligned and elongated muscle mimetic pores. As anticipated the eECM collected from these foams retained the aligned and elongated pore structure of the once underlying sacrificial foam. This was a notable finding and the first we are aware of that demonstrated the *in-vitro* collection of structured ECM. It should be possible to create sugar templates and collect ECM with architectures that mimic other structured tissues including vascular, digestive, and urogenital tissue.

The typical approach to create engineered tissues with the appropriate composition is through the use of tissue specific cell types (ex. chondrocytes = cartilage). In this study, we utilized commercially available skeletal muscle myoblasts, a well accepted cell source for skeletal muscle tissue engineering applications that also have a recognized role in the production of muscle ECM [46–48]. When grown in culture, myoblasts have been shown to produce collagen, GAGs, and other essential tissue proteins, a critical requirement for the ECM collection approach utilized in this study [49–52]. Yet, these cells did not produce overwhelmingly abundant amounts of ECM. To potentially improve eECM yield, alternatives to the myoblast could be considered. A promising alternative is the interstitial muscle fibroblast, a cell population that is broadly distributed throughout muscle tissue, can be isolated from muscle biopsy in both rats and humans, can be expanded in culture, and appears to produce muscle ECM in support of myofibers [53]. In a clinical setting, the interstitial muscle fibroblast could be harvested from healthy muscle near or even distant to the injury site during a pre-operative biopsy and then expanded in culture to create a patient specific eECM scaffold. Yet what is even more attractive is using interstitial muscle fibroblasts as a universal cell source for the fabrication of “off the shelf” eECM biomaterials. Additionally, interstitial muscle cells have been shown to contain a

subpopulation of cells with progenitor potential, and could therefore serve as both a source of ECM and cell delivery [38, 54].

In this study rat skeletal muscle ECM was characterized to establish a design template for comparison to eECM materials created using rat skeletal muscle derived cells. The use of rat muscle tissue and cells were motivated by the eventual animal model testing that is planned as the next phase of development. Ultimately, human muscle ECM properties may be required to create eECM implants targeted for clinical studies. Whether there are significant differences between human and rat muscle ECM properties is unclear, but the obvious anatomic and physiological differences between human and rats make differences likely. Similarly, muscle location (lower versus upper limb) and gender could influence ECM properties. If differences exist, it might suggest that target specific eECM or DSM implants need to be considered. Ultimately, the creation of a comprehensive human muscle ECM properties library would help guide the development of next-generation eECM materials with human ECM mimetic properties.

While we were able to demonstrate the *in-vitro* fabrication of eECM biomaterials built from the ECM collected from muscle derived cells, we recognize that these first-generation materials are not equivalent to DSM samples in all areas tested. Most notably, the mechanics and yield of eECM materials were significantly below DSM values. While the influence of these parameters on *in-vivo* performance is unclear at this point, the development of eECM materials with improved yield and mechanics is still desirable. Potentially, the further development of aligned eECM materials could improve mechanical performance. The characterization of DSM materials alongside eECM samples provided quantitative insights that will allow us to better reverse engineer skeletal muscle ECM. Moving forward, the differences between DSM materials and first-generation eECM materials that were measured in this study will provide the roadmap to direct future synthesis refinements. However, failure to achieve a perfect mimic of native muscle ECM with eECM materials is not a roadblock to *in-vivo* examination efforts. First-generation materials both support cell attachment and were well tolerated and actively remodeled by the host, key design elements that motivate further *in-vivo* examination using a peer accepted muscle regeneration animal model [55].

5. Conclusions

The key findings of this study suggest that:

1. The extracellular matrix secreted by muscle myoblasts during growth in culture can be collected to engineer a biological scaffold.
2. The eECM material contains several key extracellular matrix proteins found in native muscle ECM samples, including collagen and fibronectin.
3. While the physical properties of eECM materials are less than native muscle ECM values, the samples are durable, can be handled, and utilized as bulk filling implants.

4. The eECM material supports the attachment and proliferation of cells and is well tolerated by the host following subcutaneous implantation.
5. The eECM material can be formed into bulk networks with aligned structures similar to that observed for native muscle ECM samples

Supplementary Material

Refer to Web version on PubMed Central for supplementary material.

Acknowledgments

Research reported in this publication was supported by the National Institute Of Arthritis And Musculoskeletal And Skin Diseases of the National Institutes of Health under Award Number R15AR064481 and the Arkansas Bioscience Institute.

References

1. Hill M, Wernig A, Goldspink G. Muscle satellite (stem) cell activation during local tissue injury and repair. J Anat. 2003; 203:89–99. [PubMed: 12892408]
2. Mauro A. Satellite cell of skeletal muscle fibers. J Biophys Biochem Cytol. 1961; 9:493–5. [PubMed: 13768451]
3. Terada N, Takayama S, Yamada H, Seki T. Muscle repair after a transsection injury with development of a gap: an experimental study in rats. Scand J Plast Reconstr Surg Hand Surg. 2001; 35:233–8. [PubMed: 11680391]
4. Terzis JK, Kostopoulos VK. Free muscle transfer in posttraumatic plexopathies: part 1: the shoulder. Ann Plast Surg. 2010; 65:312–7. [PubMed: 20733367]
5. Vekris MD, Beris AE, Lykissas MG, Korompilias AV, Vekris AD, Soucacos PN. Restoration of elbow function in severe brachial plexus paralysis via muscle transfers. Injury. 2008; 39 (Suppl 3):S15–22. [PubMed: 18687429]
6. Oishi SN, Ezaki M. Free gracilis transfer to restore finger flexion in Volkmann ischemic contracture. Tech Hand Up Extrem Surg. 2010; 14:104–7. [PubMed: 20526164]
7. Guex AG, Birrer DL, Fortunato G, Tevaearai HT, Giraud MN. Anisotropically oriented electrospun matrices with an imprinted periodic micropattern: a new scaffold for engineered muscle constructs. Biomed Mater. 2013; 8:021001. [PubMed: 23343525]
8. Chen MC, Sun YC, Chen YH. Electrically conductive nanofibers with highly oriented structures and their potential application in skeletal muscle tissue engineering. Acta Biomater. 2013; 9:5562–72. [PubMed: 23099301]
9. Aviss KJ, Gough JE, Downes S. Aligned electrospun polymer fibres for skeletal muscle regeneration. Eur Cell Mater. 2010; 19:193–204. [PubMed: 20467965]
10. Ott HC, Matthiesen TS, Goh SK, Black LD, Kren SM, Netoff TI, et al. Perfusion-decellularized matrix: using nature's platform to engineer a bioartificial heart. Nat Med. 2008; 14:213–21. [PubMed: 18193059]
11. Yoo JJ, Meng J, Oberpenning F, Atala A. Bladder augmentation using allogenic bladder submucosa seeded with cells. Urology. 1998; 51:221–5. [PubMed: 9495701]
12. Seguin A, Radu D, Holder-Espinasse M, Bruneval P, Fialaire-Legendre A, Duterque-Coquillaud M, et al. Tracheal replacement with cryopreserved, decellularized, or glutaraldehyde-treated aortic allografts. Ann Thorac Surg. 2009; 87:861–7. [PubMed: 19231406]
13. Wainwright JM, Hashizume R, Fujimoto KL, Remlinger NT, Pesyna C, Wagner WR, et al. Right ventricular outflow tract repair with a cardiac biologic scaffold. Cells Tissues Organs. 2012; 195:159–70. [PubMed: 22025093]
14. Hoganson DM, Owens GE, O'Doherty EM, Bowley CM, Goldman SM, Harilal DO, et al. Preserved extracellular matrix components and retained biological activity in decellularized porcine mesothelium. Biomaterials. 2010; 31:6934–40. [PubMed: 20584548]

15. Kim MS, Ahn HH, Shin YN, Cho MH, Khang G, Lee HB. An in vivo study of the host tissue response to subcutaneous implantation of PLGA- and/or porcine small intestinal submucosa-based scaffolds. Biomaterials. 2007; 28:5137–43. [PubMed: 17764737]
16. Romano N, Sengupta D, Chung C, Heilshorn SC. Protein-engineered biomaterials: Nanoscale mimics of the extracellular matrix. Biochim Biophys Acta. 2010
17. Owen SC, Shoichet MS. Design of three-dimensional biomimetic scaffolds. J Biomed Mater Res A. 2010
18. Shekaran A, Garcia AJ. Nanoscale engineering of extracellular matrix-mimetic bioadhesive surfaces and implants for tissue engineering. Biochim Biophys Acta. 2010
19. Merritt EK, Cannon MV, Hammers DW, Le LN, Gokhale R, Sarathy A, et al. Repair of traumatic skeletal muscle injury with bone-marrow-derived mesenchymal stem cells seeded on extracellular matrix. Tissue Eng Part A. 2010; 16:2871–81. [PubMed: 20412030]
20. Wolf MT, Daly KA, Reing JE, Badylak SF. Biologic scaffold composed of skeletal muscle extracellular matrix. Biomaterials. 2012; 33:2916–25. [PubMed: 22264525]
21. Lin CH, Yang JR, Chiang NJ, Ma H, Tsay RY. Evaluation of decellularized extracellular matrix of skeletal muscle for tissue engineering. Int J Artif Organs. 2014; 0:0.
22. Nakamura RM. Monoclonal antibodies: methods and clinical laboratory applications. Clin Physiol Biochem. 1983; 1:160–72. [PubMed: 6396016]
23. Wolchok JC, Tresco PA. The isolation of cell derived extracellular matrix constructs using sacrificial open-cell foams. Biomaterials. 2010; 31:9595–603. [PubMed: 20950855]
24. Mirsadraee S, Wilcox HE, Korossis SA, Kearney JN, Watterson KG, Fisher J, et al. Development and characterization of an acellular human pericardial matrix for tissue engineering. Tissue Eng. 2006; 12:763–73. [PubMed: 16674290]
25. Liu B, Qu MJ, Qin KR, Li H, Li ZK, Shen BR, et al. Role of cyclic strain frequency in regulating the alignment of vascular smooth muscle cells in vitro. Biophys J. 2008; 94:1497–507. [PubMed: 17993501]
26. Huang NF, Lee RJ, Li S. Engineering of aligned skeletal muscle by micropatterning. Am J Transl Res. 2010; 2:43–55. [PubMed: 20182581]
27. Lasher RA, Wolchok JC, Parikh MK, Kennedy JP, Hitchcock RW. Design and characterization of a modified T-flask bioreactor for continuous monitoring of engineered tissue stiffness. Biotechnol Prog. 2010; 26:857–64. [PubMed: 20187075]
28. Wolchok JC, Brokopp C, Underwood CJ, Tresco PA. The effect of bioreactor induced vibrational stimulation on extracellular matrix production from human derived fibroblasts. Biomaterials. 2009; 30:327–35. [PubMed: 18937972]
29. Wolchok JC, Tresco PA. The isolation of cell derived extracellular matrix constructs using sacrificial open-cell foams. Biomaterials. 2010
30. Edwards CA, O'Brien WD Jr. Modified assay for determination of hydroxyproline in a tissue hydrolyzate. Clin Chim Acta. 1980; 104:161–7. [PubMed: 7389130]
31. Human organ and tissue transplantation. World Health Organization; 2003.
32. Oliva MS, Schottman T, Gulati M. Turning the tide of corneal blindness. Indian J Ophthalmol. 2012; 60:423–7. [PubMed: 22944753]
33. McGuire DA, Hendricks SD. Allograft tissue in ACL reconstruction. Sports Med Arthrosc. 2009; 17:224–33. [PubMed: 19910780]
34. Leon-Villapalos J, Eldardiri M, Dziewulski P. The use of human deceased donor skin allograft in burn care. Cell Tissue Bank. 2010; 11:99–104. [PubMed: 20077178]
35. Wolchok JC, Tresco PA. Using vocally inspired mechanical conditioning to enhance the synthesis of a cell-derived biomaterial. Ann Biomed Eng. 2013; 41:2358–66. [PubMed: 23793412]
36. Chen CZ, Peng YX, Wang ZB, Fish PV, Kaar JL, Koepsel RR, et al. The Scar-in-a-Jar: studying potential antifibrotic compounds from the epigenetic to extracellular level in a single well. Br J Pharmacol. 2009; 158:1196–209. [PubMed: 19785660]
37. Corona BT, Garg K, Ward CL, McDaniel JS, Walters TJ, Rathbone CR. Autologous minced muscle grafts: a tissue engineering therapy for the volumetric loss of skeletal muscle. Am J Physiol Cell Physiol. 2013; 305:C761–75. [PubMed: 23885064]

38. Corona BT, Ward CL, Baker HB, Walters TJ, Christ GJ. Implantation of in vitro tissue engineered muscle repair constructs and bladder acellular matrices partially restore in vivo skeletal muscle function in a rat model of volumetric muscle loss injury. Tissue Eng Part A. 2014; 20:705–15. [PubMed: 24066899]
39. Valentin JE, Turner NJ, Gilbert TW, Badylak SF. Functional skeletal muscle formation with a biologic scaffold. Biomaterials. 2010; 31:7475–84. [PubMed: 20638716]
40. Ramazanoglu M, Lutz R, Rusche P, Trabzon L, Kose GT, Prechtl C, et al. Bone response to biomimetic implants delivering BMP-2 and VEGF: an immunohistochemical study. Journal of cranio-maxillo-facial surgery: official publication of the European Association for Cranio-Maxillo-Facial Surgery. 2013; 41:826–35. [PubMed: 23434516]
41. Merritt EK, Hammers DW, Tierney M, Suggs LJ, Walters TJ, Farrar RP. Functional assessment of skeletal muscle regeneration utilizing homologous extracellular matrix as scaffolding. Tissue Eng Part A. 2010; 16:1395–405. [PubMed: 19929169]
42. de la Garza-Rodea AS, van der Velde-van Dijke I, Boersma H, Goncalves MA, van Bekkum DW, de Vries AA, et al. Myogenic properties of human mesenchymal stem cells derived from three different sources. Cell Transplant. 2012; 21:153–73. [PubMed: 21669036]
43. Bian W, Bursac N. Engineered skeletal muscle tissue networks with controllable architecture. Biomaterials. 2009; 30:1401–12. [PubMed: 19070360]
44. Lam MT, Huang YC, Birla RK, Takayama S. Microfeature guided skeletal muscle tissue engineering for highly organized 3-dimensional free-standing constructs. Biomaterials. 2009; 30:1150–5. [PubMed: 19064284]
45. Maier F, Bornemann A. Comparison of the muscle fiber diameter and satellite cell frequency in human muscle biopsies. Muscle Nerve. 1999; 22:578–83. [PubMed: 10331356]
46. Koffler J, Kaufman-Francis K, Yulia S, Dana E, Daria AP, Landesberg A, et al. Improved vascular organization enhances functional integration of engineered skeletal muscle grafts. Proc Natl Acad Sci U S A. 2011; 108:14789–94. [PubMed: 21878567]
47. Borselli C, Cezar CA, Shvartsman D, Vandenburgh HH, Mooney DJ. The role of multifunctional delivery scaffold in the ability of cultured myoblasts to promote muscle regeneration. Biomaterials. 2011; 32:8905–14. [PubMed: 21911253]
48. Riboldi SA, Sampaolesi M, Neuenschwander P, Cossu G, Mantero S. Electrospun degradable polyesterurethane membranes: potential scaffolds for skeletal muscle tissue engineering. Biomaterials. 2005; 26:4606–15. [PubMed: 15722130]
49. Wang CZ, Wang GJ, Ho ML, Wang YH, Yeh ML, Chen CH. Low-magnitude vertical vibration enhances myotube formation in C2C12 myoblasts. J Appl Physiol. 2010; 109:840–8. [PubMed: 20634357]
50. Alexakis C, Partridge T, Bou-Gharios G. Implication of the satellite cell in dystrophic muscle fibrosis: a self-perpetuating mechanism of collagen overproduction. Am J Physiol Cell Physiol. 2007; 293:C661–9. [PubMed: 17475662]
51. Miller RR, Rao JS, Burton WV, Festoff BW. Proteoglycan synthesis by clonal skeletal muscle cells during in vitro myogenesis: differences detected in the types and patterns from primary cultures. Int J Dev Neurosci. 1991; 9:259–67. [PubMed: 1927582]
52. Rao JS, Beach RL, Festoff BW. Extracellular matrix (ECM) synthesis in muscle cell cultures: quantitative and qualitative studies during myogenesis. Biochem Biophys Res Commun. 1985; 130:440–6. [PubMed: 4026839]
53. Murphy MM, Lawson JA, Mathew SJ, Hutcheson DA, Kardon G. Satellite cells, connective tissue fibroblasts and their interactions are crucial for muscle regeneration. Development. 2011; 138:3625–37. [PubMed: 21828091]
54. Corona BT, Machingal MA, Criswell T, Vadhavkar M, Dannahower AC, Bergman C, et al. Further development of a tissue engineered muscle repair construct in vitro for enhanced functional recovery following implantation in vivo in a murine model of volumetric muscle loss injury. Tissue Eng Part A. 2012; 18:1213–28. [PubMed: 22439962]
55. Wu X, Corona BT, Chen X, Walters TJ. A Standardized Rat Model of Volumetric Muscle Loss for the Development of Tissue Engineering Therapies. BioResearch Open Access. 2012:1. [PubMed: 23516669]

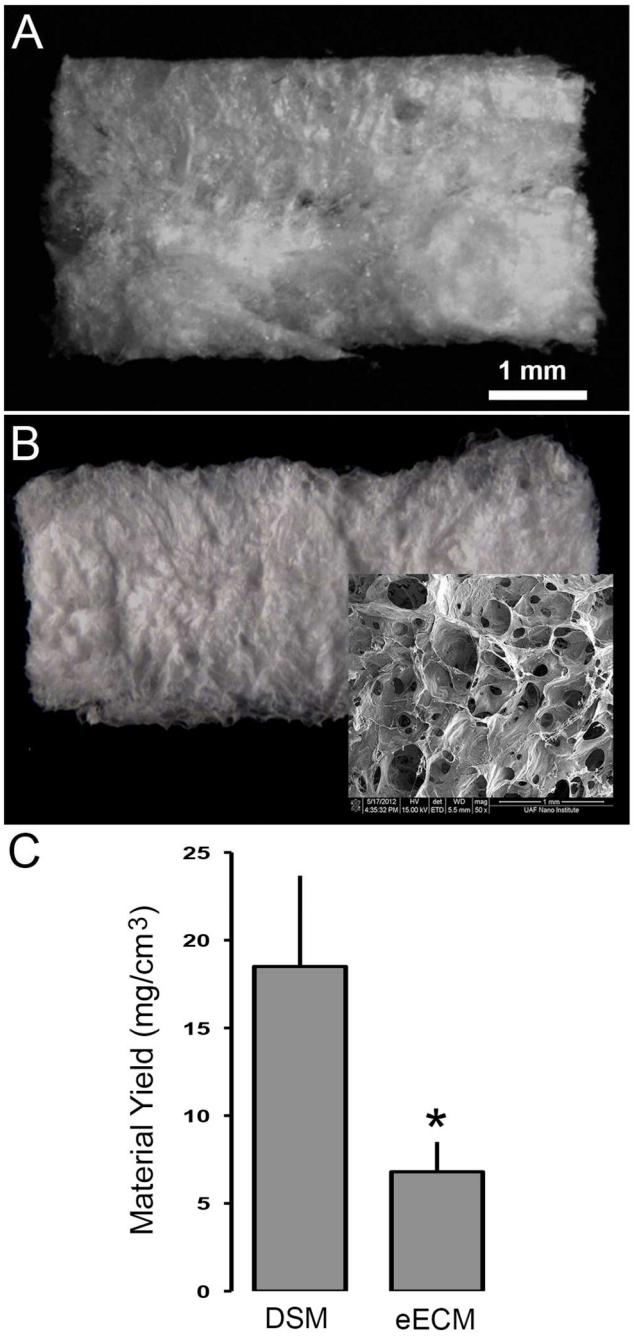

Figure 1.

Representative DSM and eECM samples prepared from either rat skeletal muscle or rat skeletal muscle myoblasts seeded onto sacrificial foams respectively (A and B). The eECM biomaterials consisted of a highly porous network with a structure that is reminiscent of the once underlying sacrificial foam (B:inset). By volume, rat muscle samples yielded three times the material of myoblast seeded sacrificial foams (C). (mean±SD; t-test $p<0.05$ n=6/ sample group)

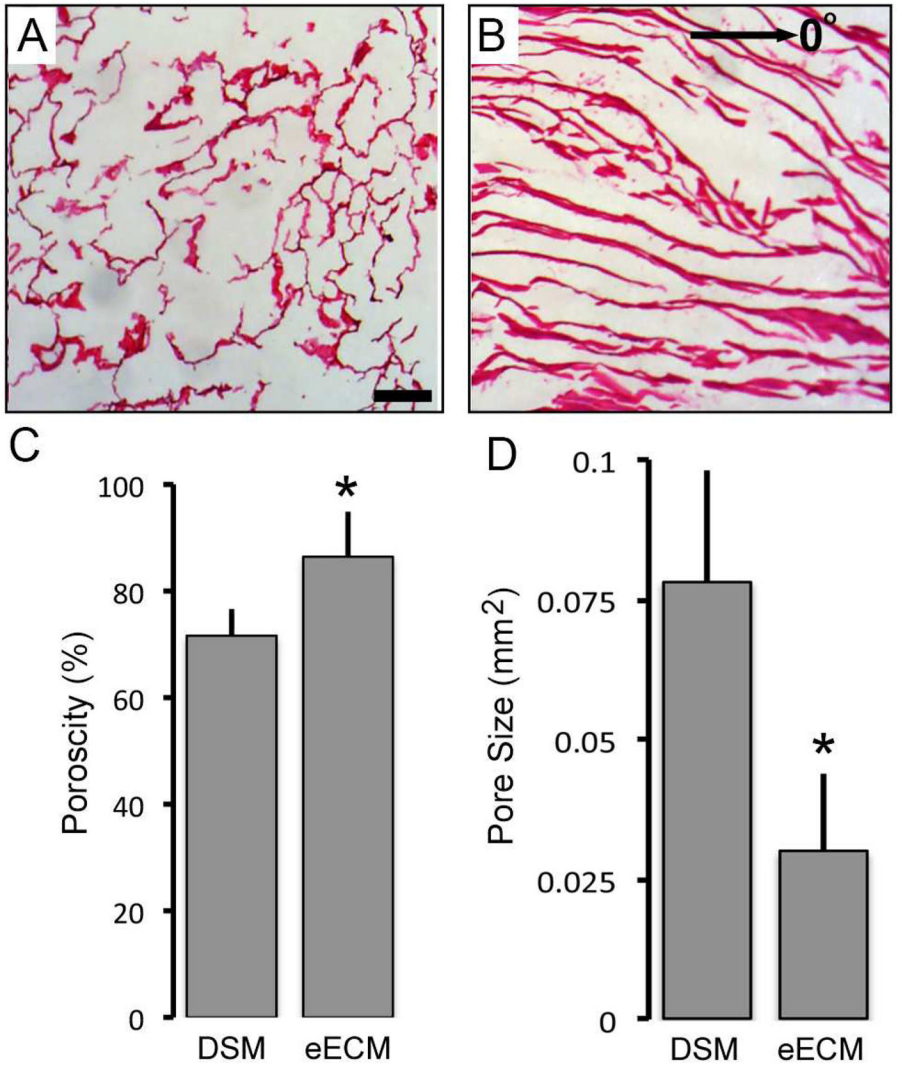

Figure 2.

Representative images of H&E stained DSM (A) and eECM (B) thin sections illustrate the porous structure, fibrillar features, and network organization. Porosity and pore size measurements revealed significant differences between eECM and DSM samples (C and D). (mean±SD; * t-test $p<0.05$ n=5/sample group)

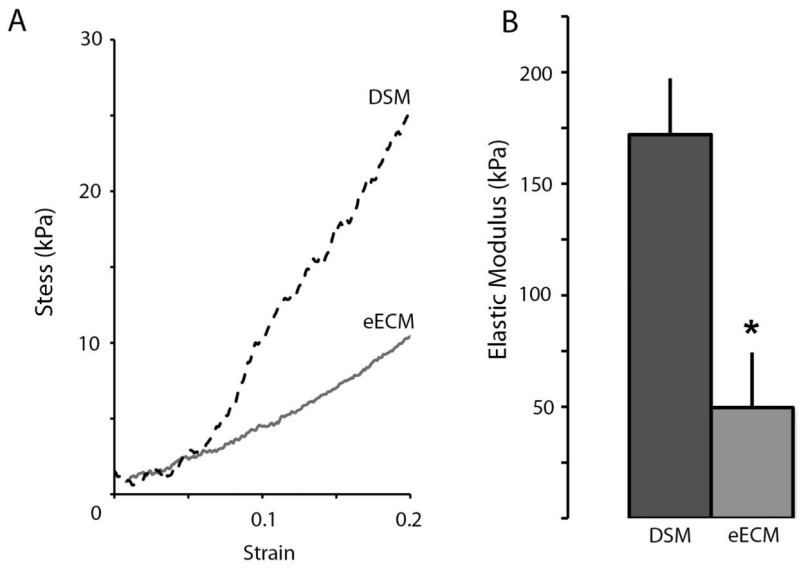

Figure 3.

Representative DSM and eECM sample stress versus strain curves (A). DSM sample elastic modulus was approximately four fold greater than eECM values (B). (mean±SD; * t-test $p<0.05$ n=4/sample group)

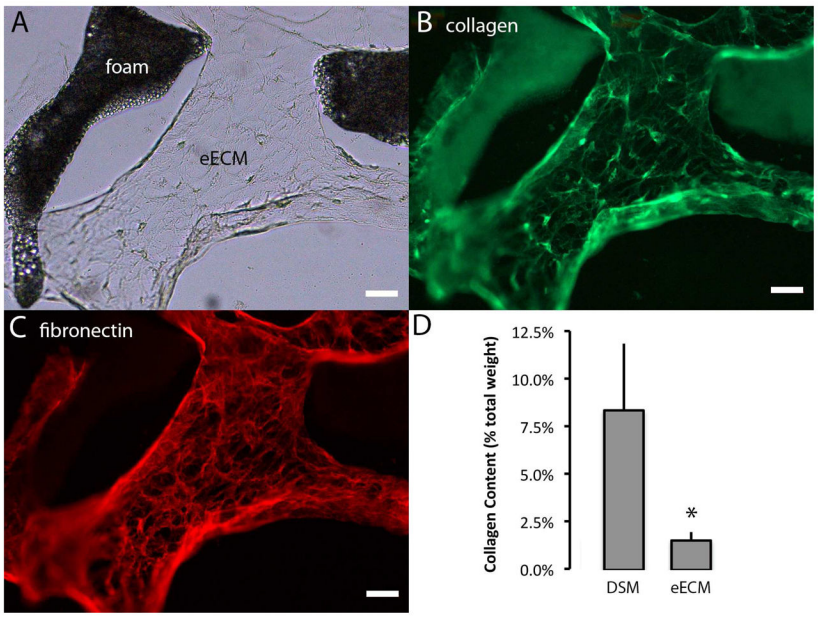

Figure 4.

Engineered ECM samples were immunostained to identify the presence of collagen type 1 (green) and fibronectin (red). The accumulated eECM biomaterial as seen with brightfield illumination (A) was immuno-reactive to both collagen type 1 (B) and fibronectin (C). The percent collagen content (dry weight) of DSM and eECM samples was estimated from hydroxy-proline concentration measurements (D). (mean±SD * t-test $p<0.05$ n=4/sample group)

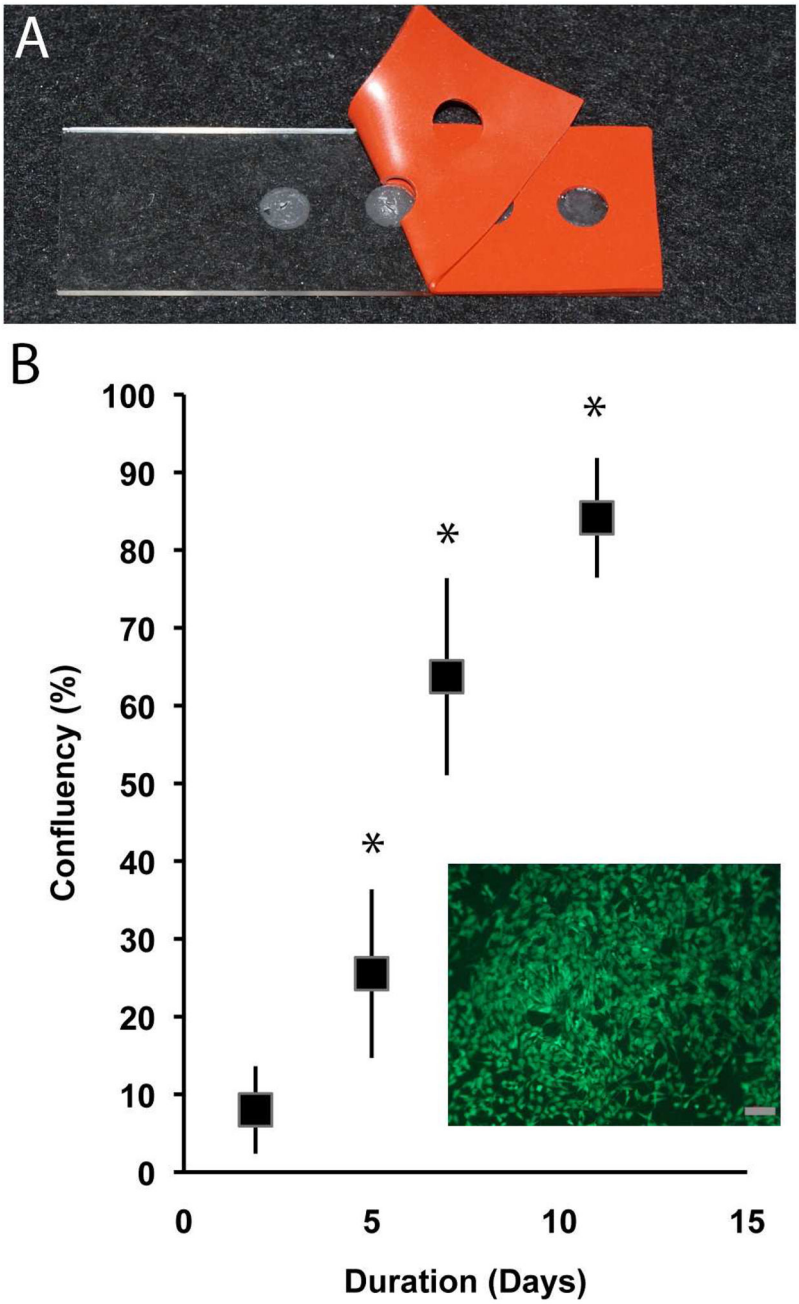

Figure 5.

Engineered ECM material islands (A) supported the attachment and proliferation (B) of viable myoblast cells (inset; scale bar =100um). The percent surface coverage was evaluated at 2, 5, 7, and 11 days post cell seeding. (mean±SD; * $p<0.05$ compared to day 2, n=4/ sample group).

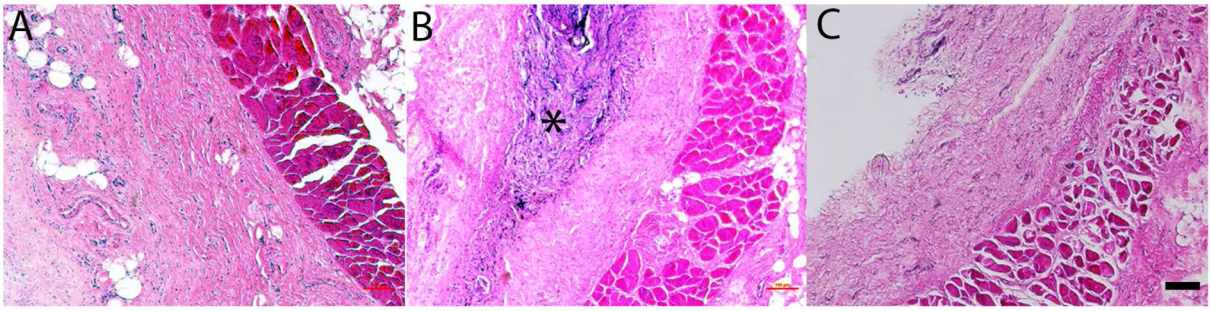

Figure 6.

Stained (H&E) thin sections collected from control (A) and eECM implanted, 4 weeks (B) and 12 weeks (C), Sprague Dawley rats. Engineered ECM biomaterials are observed within the dorsal subcutaneous implantation site at 4 weeks (*) but have been remodeled by 12 weeks in all animals tested (n=3/time point). Scale bar 100μm

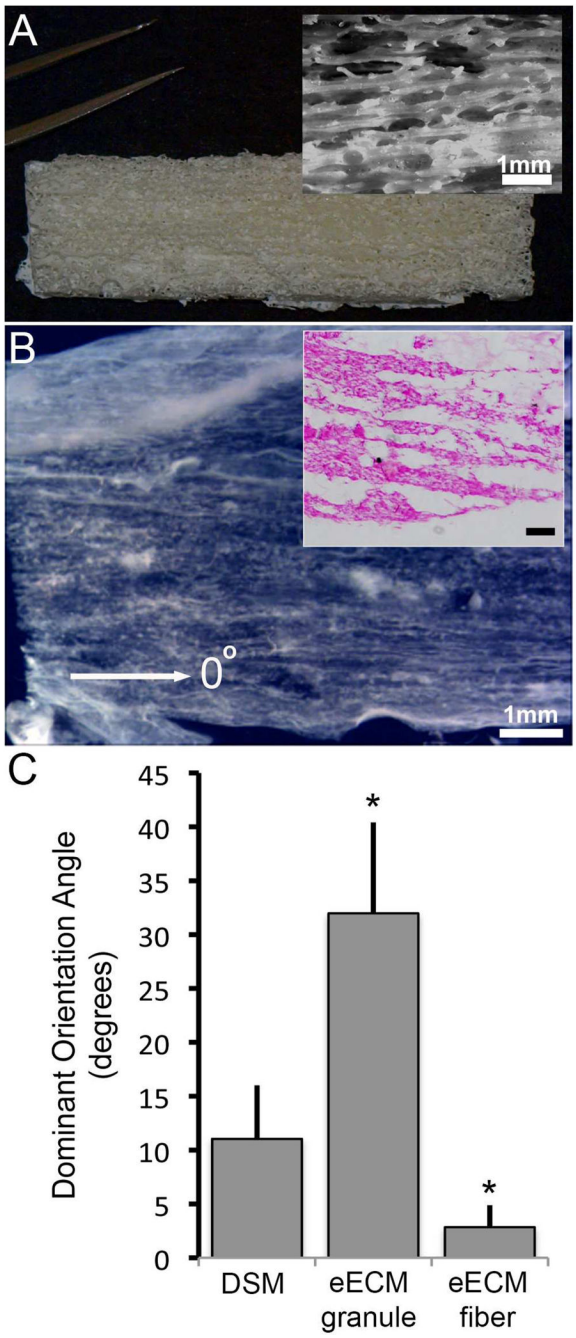

Figure 7.

The eECM collected from sacrificial foams (A) created using oriented drawn sugar fiber templates showed evidence of network alignment, which could be seen in bulk samples (B), and within histological thin sections (inset; scale bar=100um). When compared to the eECM collected from granular sugar templated foams, oriented sugar fiber eECM samples showed a greater degree of network alignment consistent with the direction of sugar fiber orientation

(defined as 0°). The network alignment was closer to that observed within DSM samples. (mean±SD; * $p<0.05$ compared to DSM samples, n=4/sample group)